International Journal of Climatology

International Journal of Climatology RMetS

RESEARCH ARTICLE OPEN ACCESS

Changing Water Resources in the Indus Basin: A Multi-Model Budyko-Based Analysis

Muhammad Arif[1] | Chia-Jeng Chen[1] | Nir Krakauer[2] | Tsung-Yu Lee[3]

[1]National Chung Hsing University, Taichung, Taiwan | [2]The City College of New York, New York, New York, USA | [3]National Taiwan Normal University, Taipei, Taiwan

Correspondence: Chia-Jeng Chen (cjchen@nchu.edu.tw)

Received: 6 February 2026 | **Revised:** 9 May 2026 | **Accepted:** 8 June 2026

Keywords: climate change | hydroclimatic variability | Indus Basin | sustainable development | water resources

ABSTRACT

Assessing hydroclimatic variability and future water availability is crucial for sustainable water-resource management. This study utilised the Budyko framework to explore baseline (1962–2005) and projected shifts in the water-energy distribution across the Indus Basin, including the Upper Indus, Kabul, Jhelum, and Chenab sub-basins. Future changes in hydroclimatic conditions were assessed using climate projections from multiple models under the RCP4.5 and RCP8.5 scenarios. Our findings highlight significant spatial variability across the Indus sub-basins: The Upper Indus demonstrated lower evaporative efficiency, whereas Chenab experienced water partitioning primarily through runoff with the highest precipitation. Kabul and Jhelum were more responsive to atmospheric evaporative demand. In both emission scenarios, all sub-basins showed noticeable changes in the Budyko space over the 21st century, mainly due to warming-induced increases in potential evapotranspiration, particularly in the Upper Indus and Chenab. The projected directions of these shifts indicate a move towards more energy-limited hydroclimatic conditions, driven by warming-induced increases in atmospheric evaporative demand across the Indus sub-basins. Ensemble projections further indicate increased hydroclimatic variability and greater sensitivity of basin-scale water distribution to the partitioning between evapotranspiration and runoff under high-emission scenarios. These results highlight the importance of effective water resource management in the Indus Basin under climate change.

1 | Introduction

Climate change intensifies hydrological uncertainty by altering rainfall patterns, evapotranspiration rates, and the distribution of water and energy across river basins (Thompson et al. 2014; Ougahi and Mahmood 2022). Rising temperatures and fluctuations in atmospheric patterns have led to substantial variations in water availability, affecting food production, hydropower, ecological processes, and water security worldwide (Lee et al. 2023). The growing need for freshwater resources, driven by climate and socioeconomic changes, necessitates the assessment of long-term water-balance dynamics at the basin scale to evaluate future water security and mitigation needs (Siegfried et al. 2024).

Among the many approaches for assessing the impacts of climate and watershed characteristics on water distribution, Budyko-based analysis, which is based on the relationship between long-term precipitation (P), potential evapotranspiration (PET), and actual evapotranspiration (AET), offers a robust and physically grounded framework (Wang et al. 2016; Xu et al. 2022). Owing to its conceptual simplicity and ease of interpretation, the Budyko framework, including an evaporative index (AET/P) and aridity index (PET/P), has been widely applied across diverse climatic and geographic regions, including arid, humid, and snow-dominated basins. In this study, the selected sub-basins represent distinct hydroclimatic regimes, including glacier-dominated headwaters in the Upper Indus, semi-arid conditions in the Kabul basin, and monsoon-influenced environments in the Jhelum and Chenab basins. Despite this climatic distinction, the Budyko framework has been shown to provide a robust first-order description of long-term water–energy partitioning across diverse climatic and physiographic settings (Berghuijs et al. 2017, 2020; Gnann et al. 2019). Previous studies have demonstrated its applicability across arid and semi-arid regions (Wang and Tang 2014; Zhang et al. 2008), as well as tropical and temperature-gradient environments, including snow- and elevation-influenced catchments (Li et al. 2013; Maurer et al. 2022; Trancoso et al. 2016). In contrast to process-based hydrological models, which require extensive parameterisation of land-surface processes and detailed meteorological data, the Budyko framework offers a simplified method for assessing long-term water balance at the basin scale. This feature makes Budyko-type analyses especially appropriate for large river basins and data-scarce mountainous areas where hydrological observations and model parameter constraints are often limited (Greve et al. 2020; Koppa and Gebremichael 2017). Furthermore, the Budyko framework has been enhanced by incorporating key parameters and variables, including a catchment-specific Fu exponent (ω) and measures of the extent and direction of basin-scale changes in Budyko space. This enhanced Budyko-based framework has been used to evaluate hydroclimatic variability and assess future water availability under climate change (Lee et al. 2023). Budyko-based analyses have been used to elucidate changing water cycles in Taiwan, the Ganga Basin, the Canadian Shield, and the Yangtze River Basin (Lee et al. 2026; Sun et al. 2025; Wang et al. 2025; Zhang et al. 2025). In this context, the Budyko framework provides a practical approach for assessing climate-driven changes in basin-scale water availability and hydrological partitioning in large river systems.

The Indus River Basin (IRB) ranks among the most hydroclimatically sensitive and socioeconomically vital river systems globally, spanning Pakistan, India, Afghanistan, and China, and supporting more than 300 million people (Khan and Adams 2019; Asghar et al. 2019). This basin is heavily dependent on snow and glacier melt and supports one of the largest irrigation networks globally, with over 95% of its water resources dedicated to agriculture (Yang et al. 2014). Hydrological variability within the IRB is mainly influenced by two major atmospheric circulation patterns: the South Asian summer monsoon and mid-latitude winter westerlies, which together create significant spatial and seasonal differences in temperature, precipitation, and runoff. Annual precipitation varies from less than 400 mm in the dry lower plains to more than 1000–1500 mm in the northern high-altitude regions (Munchak et al. 2022). The Upper Indus Basin alone accounts for approximately 70% of the basin's total annual flow, with approximately 26% from glacier melt and 44% from seasonal snowmelt, highlighting the essential role of cryospheric processes in ensuring downstream water availability (Jamshed et al. 2025). Streamflow typically peaks between July and September because of the combined effects of monsoon rainfall and meltwater. Recent evidence indicates that intensified monsoon activity leads to increased rainfall extremes in southern Punjab and northern Sindh, exacerbating the flood frequency and hydroclimatic variability (Atif et al. 2021; Luo et al. 2024).

Although there has been significant research on the effects of climate change in the IRB using runoff modelling, degree-day melt techniques, and process-based hydrological models, these approaches often require extensive calibration, are highly sensitive to limited high-altitude data, and provide only a limited understanding of the long-term water-energy distribution at the basin scale (Archer and Fowler 2004; Rajbhandari et al. 2015; Mukhopadhyay and Khan 2015). Process-based modelling studies frequently encounter constraints related to data scarcity, calibration uncertainty, and concentrated examination of individual sub-basins or historical time periods. Consequently, existing assessments often emphasise localised hydrological behaviour rather than providing an integrated picture of long-term water–energy partitioning across the entire IRB, particularly when evaluated under multiple climate model projections (Demeke et al. 2025). This limitation is more pronounced in hydroclimatically diverse basins, such as the IRB, where strong elevation gradients, cryospheric influences, and spatially heterogeneous precipitation regimes complicate the interpretation of future water availability.

Furthermore, only a limited number of studies have employed basin-wide, multi-model regional climate projections to evaluate future hydroclimatic changes throughout the Indus River system (Saha et al. 2020; Shafeeque et al. 2022). Some earlier evaluations of future hydrology in the IRB have depended on global climate model outputs with coarse resolution and minimal bias correction, even though there is substantial evidence that the basin's intricate topography and significant orographic gradients require high-resolution, regionally downscaled climate data for accurate hydroclimatic assessments (Kotamarthi et al. 2021; Shah et al. 2024).

This study addressed these constraints by utilising the Budyko framework alongside bias-corrected, high-resolution climate simulations from CORDEX South Asia to investigate both baseline and future hydroclimatic variability in significant sub-basins of the IRB. By focusing on the relationship between water and energy fluxes aggregated at the basin level rather than on detailed process modeling, this method offers a physically coherent and comprehensive overview of long-term hydroclimatic changes and future water availability in the Indus Basin.

The specific objectives of this work are as follows:

- To quantify the projected changes in aridity and evaporative index across the Kabul, Upper Indus, Jhelum, and Chenab basins under the RCP4.5 and RCP8.5 scenarios, utilising a Budyko-based framework with catchment-specific Fu parameters (ω) computed from the baseline period.
- To assess the relative contributions of variations in precipitation and potential evapotranspiration to anticipated variations in water balance, utilising change components.
- To evaluate inter-model uncertainty and spatial variability in the projected hydrological responses. This study addresses existing gaps by performing a comprehensive basin-wide analysis based on the Budyko framework and using multiple climate models to evaluate baseline and future shifts in water and energy distribution throughout the

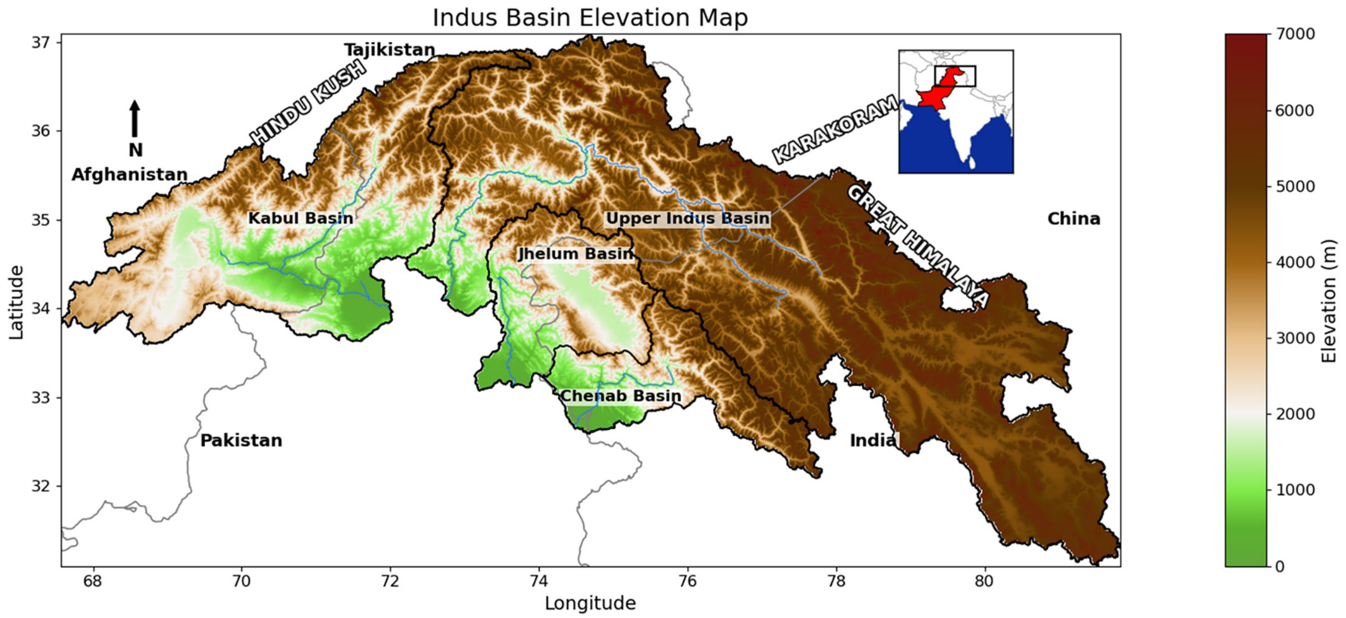

FIGURE 1 | Elevation map of the Indus Basin delineating the Upper Indus, Kabul, Jhelum, and Chenab sub-basins and international boundaries. [Colour figure can be viewed at wileyonlinelibrary.com]

Indus Basin. Thus, this study offers a perspective on future hydroclimatic risks and water availability, which is pertinent to irrigation planning, transboundary water management, and climate adaptation in the Indus Basin.

The remainder of this paper is structured as follows: Section 2 outlines the study area and datasets employed. Section 3 presents the methodological framework. Section 4 details the historical and projected hydroclimatic results. Section 5 discusses the implications and uncertainties, and Section 6 summarises the main conclusions.

2 | Materials

2.1 | Study Area

The IRB is a cross-border system that spans Pakistan, India, Afghanistan, and China, supplying water to more than 300 million people through the world's most extensive irrigation network (Sattar and Kinouchi 2025). The river flows 2682 km within Pakistan (Sarwar et al. 2026). Every year, approximately 122 km^3 of surface water is diverted for agriculture, and more than 95% of the available water is used for irrigation (Laghari et al. 2012; Muzammil et al. 2020; Qureshi and Perry 2021). The basin's already limited water supply is under increasing pressure as the population is expected to grow from 300 million in 2020 to approximately 383 million by 2050. The basin has experienced a wide range of climatic and geological changes.

The lower Indus Plains, located in the southern part of the Indus Basin, are predominantly positioned below 200 m above the mean sea level, whereas the Himalayan-Karakoram headwater regions rise over 7000 m above the mean sea level (Dubey et al. 2023). The HydroSHEDS digital elevation model (DEM, Lehner et al. 2008), which is frequently used for large-scale hydrological assessments and is based on hydrologically conditioned SRTM elevation data, was used to determine basin boundaries and elevation parameters (Figure 1). These elevation gradients significantly affect regional hydroclimatic processes. Orographic influences determine the spatial distribution of precipitation, whereas snow and glacier melt play a dominant role in sustaining streamflow in the higher regions of the basin (Kan et al. 2018; Hussain et al. 2022). We chose four sub-basins of the Indus Basin for the study: the Upper Indus Basin (UIB), Kabul, Jhelum, and Chenab. These four sub-basins were selected based on their distinct hydroclimatic characteristics, availability of stream gauge data, and significant contributions to the overall discharge of the Indus Basin. This makes them essential for analyzing water availability across basins in the context of climate change. The Upper Indus Basin is mainly affected by snow and ice melt, the Kabul Basin is mainly affected by winter westerly disturbances, and the Chenab and Jhelum rivers mostly receive rain during the summer monsoon season, creating a mixed nival-pluvial runoff regime (Dahri et al. 2021; Giese et al. 2022; Latif et al. 2021; Yaseen et al. 2022). The hydroclimate of the Indus Basin is affected by two main circulation patterns: the South Asian summer monsoon, which occurs from June to September, and mid-latitude westerly disturbances, which occur from December to April (Dimri et al. 2019; Riley et al. 2021; Hussain et al. 2023). The area receives annual precipitation ranging from less than 200 mm in the dry lowlands to 2000 mm at higher altitudes (Krakauer et al. 2019). The average yearly temperature ranges from less than 0°C in glacial areas to more than 25°C in the plains.

The CORDEX South Asia simulations project significantly rising air temperatures throughout the Indus Basin. Warming is particularly pronounced in high-altitude regions, including the study sub-basins (Liu and Chen 2000; Ougahi and Mahmood 2022; Chatterjee 2024). Changes in precipitation will vary by location, and runoff shifts could exceed 100% depending on the elevation, scenario, and time (Dimri et al. 2019; Dubey et al. 2023; Mondal et al. 2021). These expected changes make it difficult to predict the amount of water available in the future, underscoring the importance of hydrological assessments and adaptation strategies at the basin level.

2.2 | Data

2.2.1 | Precipitation

In this study, ERA5 was selected as the primary precipitation dataset after considering several other gridded precipitation datasets, including CRU TS and GPCC, which, by comparison between the derived and observed streamflow data, were found to underestimate precipitation in the high-altitude regions of the Indus Basin (Dahri et al. 2021). The baseline precipitation across the study area (averaged within each sub-basin) was derived from the ERA5 reanalysis of the European Center for Medium-Range Weather Forecasts (ECMWF). ERA5 is a fifth-generation global reanalysis that employs 4-dimensional variational data assimilation of observations from various sources to produce physically consistent atmospheric and land-surface variables (Liaqat et al. 2022; Rakhmatova et al. 2021). ERA5 monthly precipitation data from 1962 to 2005 were obtained at a 0.25° resolution and converted to basin-mean values. ERA5 has been shown to capture spatial and seasonal variations in precipitation trends in the Indus, outperforming other gridded datasets in high-altitude regions (Dahri et al. 2021; Liaqat et al. 2022). Therefore, ERA5 data were used as an observational benchmark for bias-correcting the CORDEX model simulations and as the baseline precipitation input for the Budyko computations. Further support for using ERA5 as the reference precipitation dataset came from a basin-scale water-balance assessment using GPCC precipitation, which also gave physically contradictory AET values in the headwater basins (Table S1).

2.2.2 | Temperature

The baseline temperature CRU TS dataset provides monthly average air temperatures derived from global-station observations (Harris et al. 2020). The duration is substantial, making it suitable for assessing climate variations and conducting trend analysis. The CRU data were available at a spatial resolution of 0.5°×0.5°. The CRU TS temperature data were regridded from 0.5° to 0.25° resolution using bilinear interpolation with Climate Data Operators (CDO), which aligned with other climate datasets.

2.2.3 | Observed Streamflow

Daily streamflow data for the Upper Indus, Kabul, Jhelum, and Chenab sub-basins from 1962 to 2005 were obtained from Ali et al. (2023). These data were compiled and quality-checked using records from the Global Change Impact Studies Center (GCISC) in Pakistan. The selected gauging stations are located upstream of major reservoir control structures, ensuring that the streamflow data represent near-natural flow conditions with minimal anthropogenic regulation. The analysis period was limited to 1962 onward to ensure data consistency, as earlier records contained incomplete observations (e.g., 1961). No interpolation or infilling was applied; instead, only complete and consistent records were used. The dataset, which reflects basin-scale discharge from in situ gauging stations, served as the observational foundation for the runoff and water balance analyses in this study.

2.2.4 | CORDEX South Asia

Future climate predictions were sourced from the CORDEX South Asia regional simulations conducted over the WAS-44 domain (a standard CORDEX South Asia domain with a horizontal resolution of 0.44°). The Indian Institute of Tropical Meteorology (IITM) performed dynamic downscaling using the RegCM4-4 regional climate model. The boundary conditions were sourced from six CMIP5 global climate models (CCCma-CanESM2, GFDL-ESM2M, IPSL-CM5A-LR, MPI-ESM-MR, CNRM-CM5, and CSIRO-Mk3-6-0), which were chosen to cover a broad spectrum of climate sensitivities and model frameworks (Iqbal et al. 2017; Kumar and Dimri 2018; McSweeney et al. 2012; Sa'adi et al. 2020). Two greenhouse gas emission scenarios, namely RCP4.5 and RCP8.5, were evaluated to demonstrate stabilisation and high-emission trajectories, respectively. The downscaled CORDEX simulations provide a clearer understanding of the region and how monsoons and westerlies interact compared to lower-resolution GCM outputs, making them useful for hydroclimatic evaluations at the basin level (Choudhary and Dimri 2018).

3 | Methods

3.1 | Bias Correction of Climate Model Outputs

To rectify systematic biases in the precipitation and temperature outputs from the CORDEX regional climate simulations, we used the Empirical Quantile Mapping (EQM) technique (Cannon et al. 2016; Tong et al. 2021). This method matches the cumulative distribution functions (CDFs) of the modelled variables to those of the reference observations, thereby modifying both the average state and the distributional features. In this study, ERA5 and CRU TS were used as reference datasets for precipitation and temperature. Bias correction was performed separately for each month of the year and for each of the six CORDEX simulations over the baseline period from 1962 to 2005. The mapping functions developed from these historical data were subsequently applied to future projections under the RCP4.5 and RCP8.5 scenarios.

The EQM approach used in this research employs a non-parametric method, and the adjustment is obtained directly from the empirical CDFs of both the modelled and reference datasets. This method has been extensively demonstrated to be adaptable and efficient at minimising systematic biases in precipitation and temperature, particularly in regional climate simulations and in complex-terrain regions (Gudmundsson et al. 2012; Cannon et al. 2015; Chen et al. 2022). A sample EQM Python script is provided in Supporting Information.

Bias correction was conducted on a monthly basis with no specific adjustment to wet-day frequency, as the main goal was to address distributional features and seasonal climate patterns. Values that fell outside the calibration range were kept within the historical modelled distribution to prevent unrealistic extrapolation. Extensive calibration is carried out using data spanning from 1962 to 2005, which offers a solid foundation for establishing stable empirical relationships (Holthuijzen et al. 2022). The effectiveness of the bias correction was assessed by comparing the unadjusted and adjusted precipitation data with the reference dataset (Figures S1 and S2), which showed better alignment with seasonal climatology.

It is recognised that traditional quantile mapping techniques do not naturally preserve trends, especially concerning higher-order moments and extreme values (Cannon et al. 2015; Holthuijzen et al. 2022). Alternatively, EQM is employed to enhance the depiction of past precipitation patterns before conducting hydroclimatic analysis. The findings are evaluated at the annual and basin levels within the Budyko framework, rather than focusing on variations in extreme events (Ngai et al. 2017; Rao et al. 2022; Saha et al. 2025). Once bias-corrected, the multi-model means of the six CORDEX simulations were used to compute hydroclimatic indices (PET/P and AET/P) and to estimate model uncertainty by averaging across multiple models.

3.2 | Potential Evapotranspiration and Runoff

In this study, the Thornthwaite method (Thornthwaite 1948) was employed to estimate potential evapotranspiration (PET) using monthly average temperatures, which were computed in Python using the PyETo package (see Supporting Information) to ensure a consistent and reproducible computational approach (Trajkovic 2005; Vremec et al. 2024). The Thornthwaite method relies solely on air temperature and day length, making it particularly suitable for large-scale hydroclimatic evaluations in regions with limited data and high altitudes, where observations of radiation, wind speed, and humidity are scarce or unreliable (Aschonitis et al. 2022; Oliveira-Aparecido et al. 2021). Previous research has shown that the Thornthwaite method is favored in data-scarce regions and has been effectively utilised in Pakistan and similar semi-arid regions to estimate PET and aridity variability (Ahmed et al. 2019; Zarch et al. 2015). Furthermore, assessments suggest that temperature-based PET estimates derived from the Thornthwaite method are as accurate as more data-intensive approaches when applied over monthly to annual time frames in basin-scale studies (Dallaire et al. 2021; Aschonitis et al. 2022; Kuo et al. 2024; Lee et al. 2023). Considering the sparse meteorological network, intricate topography, and vast high-altitude regions of the Indus Basin, the Thornthwaite method offers a reliable and suitable foundation for estimating PET within the Budyko framework, where the focus is on the relative variations in PET/P and AET/P rather than the absolute evapotranspiration values (Shaw and Riha 2011; Santos et al. 2024). The current study emphasises basin-scale hydroclimatic partitioning within the Budyko framework, utilising long-term yearly variables, where PET mostly signifies climatic evaporative demand instead of intricate surface energy fluxes.

The Thornthwaite method for calculating PET uses the following equation:

$$PET = 16\left(\frac{L}{12}\right)\left(\frac{N}{30}\right)\left(\frac{10T_m}{I}\right)^a \tag{1}$$

where PET is measured in mm/month, and L represents the average day length (in hours; Thornthwaite 1948; Li et al. 2022; Xu et al. 2022; Lee et al. 2023), N is the number of days in the month, T_{m} (°C) is the monthly average temperature, and I is the annual heat index (dimensionless), defined as:

$$I = \sum_{i=1}^{12}\left(\frac{T_i}{5}\right)^{1.514} \tag{2}$$

$$a = \left(6.75\times10^{-7}\right)I^3 - \left(7.71\times10^{-5}\right)I^2 + \left(1.792\times10^{-2}\right)I + 0.49239 \tag{3}$$

where T_i (°C) represents the mean temperature of month i. Following the Thornthwaite based standard, monthly temperatures below 0°C were set to zero prior to calculating the heat index to avoid non-physical values in cold conditions. PET was initially calculated at the monthly time step and subsequently aggregated to annual totals for each grid cell. During the baseline period, AET was determined using the water balance equation as follows:

$$Q = P - AET + \Delta S \tag{4}$$

For this study, observed streamflow data were collected from gauging stations managed by the Global Change Impact Studies Center (GCISC) across the four sub-basins for the baseline period (Ali et al. 2023).

$$\overline{AET} = \overline{P} - \overline{Q} \tag{5}$$

where P is the average amount of rain that falls over the basin, as measured by ERA5 reanalysis data, provided at a monthly temporal resolution, was aggregated to annual totals to ensure consistency with PET and runoff in the Budyko analysis. Q is the observed runoff (mm/month), which was derived from the streamflow records (m^3/s), the basin areas used for runoff conversion correspond exactly to the delineated upstream catchments of the gauging stations, ensuring consistency with the spatial averaging of precipitation and PET.

$$Q_{(\text{mm/day})} = \frac{Q_{(m^3/s)} \times \ 86400}{A} \times 1000 \tag{6}$$

where $Q_{(\text{mm/day})}$ represents the runoff depth, while A represents the drainage area of the basin expressed in m^2. The calculated runoff depths were subsequently aggregated to monthly totals. The calculated runoff depth values were aggregated to monthly totals, which were then summed to obtain the annual runoff totals. We used temperature and precipitation projections from the bias-corrected CORDEX RegCM4-4 GCM models to predict future PET and aridity levels. Using the Budyko framework, we calculated future AET by combining the projected PET/P ratio with the catchment-specific Budyko parameter (ω), which was estimated from the baseline period and assumed to be constant for future projections. This analysis was conducted for both the near-term (2021–2040) and

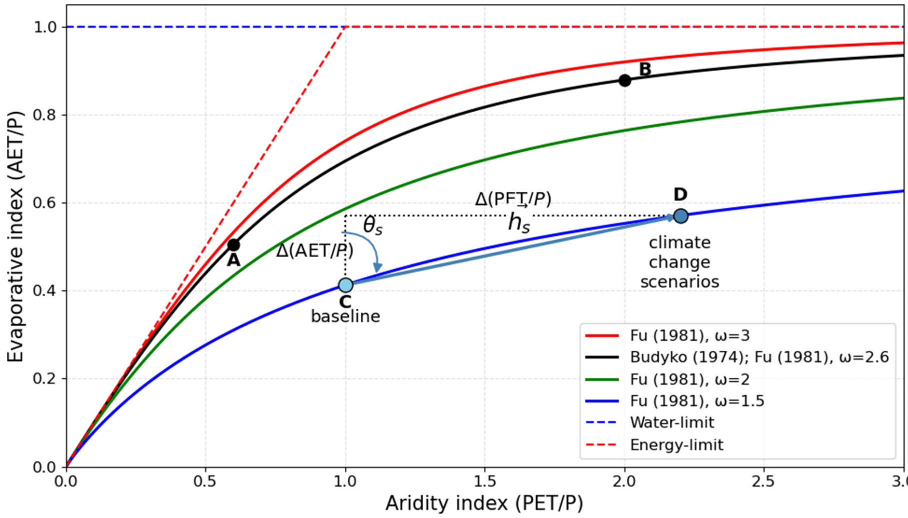

FIGURE 2 | Conceptual diagram illustrating the Budyko space, showing the parametric Fu (1981) curves for different ω values. Points A and B represent humid and arid catchments, respectively. The vector $\overrightarrow{hs}$ illustrates the shift in hydroclimatic conditions from the baseline (C) to the future scenario (D), with Is denoting the magnitude and Θs the direction of change. The blue dashed line represents the water limit (AET/p = 1), whereas the red dashed line shows the energy-limited boundary. [Colour figure can be viewed at wileyonlinelibrary.com]

far-term (2081–2100) periods under the RCP4.5 and RCP8.5 scenarios (Lee et al. 2023).

3.3 | Budyko Framework, Indices and Parameter Estimation

In the Budyko framework, hydroclimatic conditions are described using two dimensionless indices: the aridity index (PET/P), which indicates the atmospheric demand for evapotranspiration compared to water availability, and the evaporative index (AET/P), which measures the proportion of precipitation lost through evapotranspiration. Additionally, the parameter ω in Fu's formulation accounts for catchment effects by incorporating variations in water and energy partitioning that may be due to basin characteristics such as vegetation, soil properties, and topography. Thus, we considered precipitation (P), potential evapotranspiration (PET), actual evapotranspiration (AET), and runoff (R) as hydroclimatic variables; PET/P and AET/P as derived dimensionless indices; and ω as a model parameter.

The original Budyko curve is an empirical relationship typically approximated over long periods in large river basins (Wang et al. 2016) (Figure 2) based on the equilibrium between water availability and atmospheric demand. Various points along this curve indicate different hydroclimatic conditions: catchments in humid areas tend to approach the energy-limited boundary, whereas those in arid areas lean towards the water-limited boundary. These boundaries are associated with aridity indices (PET/P) that are less than or greater than 1, respectively.

$$\frac{AET}{P} = \sqrt{\frac{PET}{P} tanh\left(\frac{PET}{P}\right)^{-1}\left(1 - \exp\left(-\frac{PET}{P}\right)\right)} \tag{7}$$

The original Budyko equation (Equation 7) links the evaporative index (AET/P) with the aridity index (PET/P) in a relationship that is valid for any watershed. Many attempts have been made to enhance their relevance by integrating basin-specific features. Notably, Fu (1981) suggested a modified version of the Budyko equation, incorporating a catchment-specific parameter (ω) to reflect the combined effects of climate, topography, vegetation, and soil characteristics on the long-term water balance, as detailed by Feng et al. (2025):

$$\frac{AET}{P} = 1 + \frac{PET}{P} - \left[1 + \left(\frac{PET}{P}\right)^{\omega}\right]^{\frac{1}{\omega}} \tag{8}$$

To better capture the inter-catchment variability in the interrelationship of water and energy fluxes, this modified Budyko formulation was used in this study.

3.4 | Hydroclimatic Shift Metrics in the Budyko Space

In this study, hydroclimatic changes between the baseline and future periods were evaluated as the displacement of each subbasin in Budyko space. The magnitude of the shift (Equation 9) quantifies the distance between the baseline and future Budyko coordinates, representing the overall intensity of hydroclimatic change. The shift direction (Equation 10) is defined in the $\Delta\varphi - \Delta\varepsilon$ space, measured clockwise from the positive $\Delta\varepsilon$ axis (positive y-axis), where φ = PET/P and ε = AET/P. Accordingly, θ_s values between 0° and 90°show concurrent increase in both aridity ($\Delta\varphi > 0$) and evaporative ($\Delta\varepsilon > 0$), corresponding to a northeastward shift in Budyko space.

$$I_s = \left|\overrightarrow{h_s}\right| = \sqrt{\left(\Delta\frac{PET}{P}\right)^2 + \left(\Delta\frac{AET}{P}\right)^2} \tag{9}$$

$$\theta_s = b - \left(\left(\arctan\frac{\Delta\frac{AET}{P}}{\Delta\frac{PET}{P}}\right) \times \frac{180}{\pi}\right) \tag{10}$$

b = 90° when Δ(PET/P) > 0, and b = 270° when Δ(PET/P) < 0. Other quadrants correspond to different combinations of

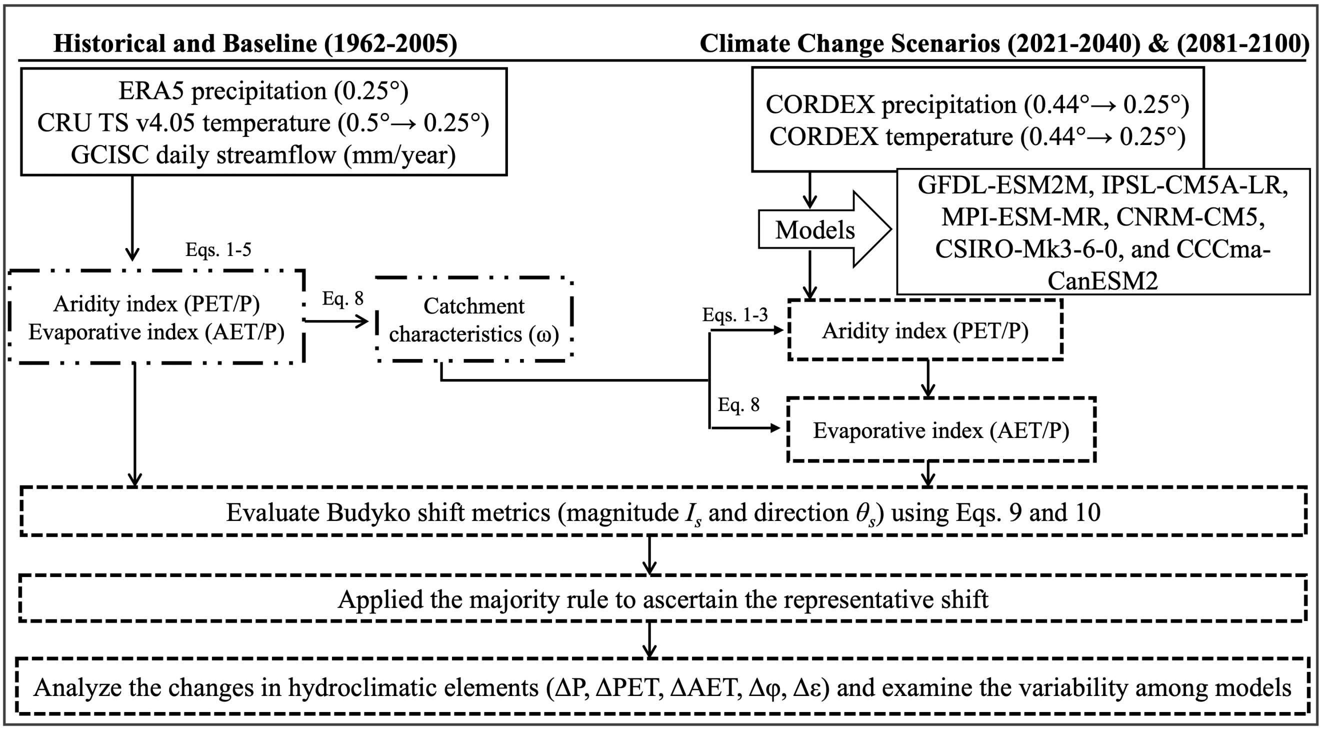

FIGURE 3 | The methodological framework for Budyko-based hydroclimatic analysis, consisting of data sources, index computation, and shift metrics under both scenarios.

changes in φ and ε. This formulation provides a consistent geometric interpretation of hydroclimatic shifts in Budyko space and ensures consistency across all figures.

To identify the dominant climatic and evaporative drivers of Budyko shifts, changes in precipitation (ΔP), potential evapotranspiration (ΔPET), and actual evapotranspiration (ΔAET) were analyzed together with their derived indices ($\Delta\varphi = \Delta(\text{PET/P})$ and $\Delta\varepsilon = \Delta(\text{AET/P})$). The ensemble means and standard deviations were computed across the six bias-corrected CORDEX-RegCM4-4 models for each sub-basin and scenario. Variations between the Δ components derived from different climate models were used to quantify model uncertainty and interpret the physical mechanisms underlying hydroclimatic shifts in Budyko space.

Figure 3 presents a schematic representation of the overall framework of this study. It shows the data sources, computation of the Budyko index, and assessment of hydroclimatic shift metrics under both the baseline and projected climate scenarios.

4 | Results

4.1 | Baseline Hydroclimatic Characteristics

Figure 4 illustrates the fundamental Budyko characteristics of the four Indus sub-basins (UIB, Kabul, Jhelum, and Chenab) from 1962 to 2005, and Table 1 lists related Budyko parameters. The relationship between the aridity index (PET/P) and evaporative index (AET/P) highlights distinct hydroclimatic patterns across the basins in the study area. Under similar aridity conditions, Kabul and Jhelum exhibited relatively higher evaporative indices. The UIB and Chenab showed lower AET/P values, suggesting that the latter basins exhibited a lower evaporative fraction and more runoff-dominated partitioning. The calculated ω parameter values highlight distinct differences in long-term water and energy distribution across the Indus sub-basins, underscoring the combined effects of factors such as topography, cryospheric impacts, and land-surface characteristics. These baseline distinctions also serve as references for assessing future climate-driven changes in each sub-basin.

In the baseline period, the Kabul and Jhelum sub-basins were categorised by higher evaporative indices, with the Jhelum sub-basin showing higher precipitation. In contrast, the Upper Indus Basin and Chenab exhibited lower AET/P ratios, indicating different controlling factors. The Upper Indus is more constrained by water and energy, whereas the Chenab is characterised by high runoff and a lower evaporative fraction. The differences in the estimated ω parameter emphasise the distinct catchment characteristics of the Indus sub-basins.

4.2 | Projected Hydroclimatic Shifts in the Budyko Space Under RCP4.5 and RCP8.5

Figure 5 illustrates the representative Budyko shifts for the four Indus sub-basins during the near-future and long-term periods under the RCP4.5 and RCP8.5 scenarios. The direction of each arrow indicates the shift angle (θ_s), whereas its length and colour reflect the magnitude of change (I_s). In the context of RCP4.5 (Figure 5a,b), all sub-basins showed a slight shift towards the northeast in the Budyko space, indicating simultaneous increases in precipitation (P) and potential evapotranspiration (PET). The extent of this change is relatively

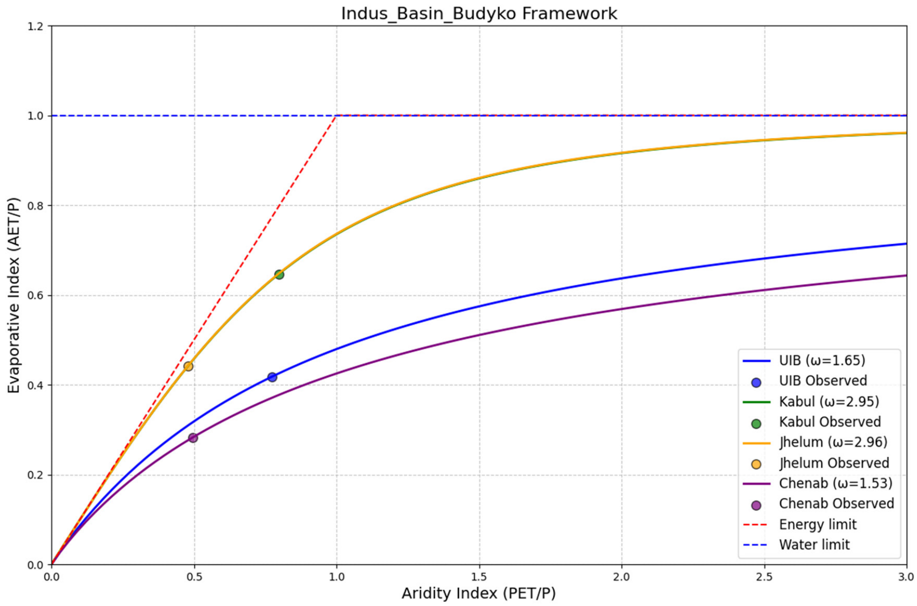

FIGURE 4 | Baseline Budyko distribution of the four Indus sub-basins with fitted Fu's ω values. [Colour figure can be viewed at wileyonlinelibrary.com]

TABLE 1 | Basin-averaged baseline hydroclimatic variables and Budyko parameters for the Indus sub-basins from 1962 to 2005.

Rivers	R (mm/year)	P (mm/year)	PET (mm/year)	ω	PET/P	AET/P	AET (mm/year)
UIB	445.09	764.67	591.18	1.65	0.78	0.41	319.52
Kabul	287.33	815.26	650.17	2.95	0.79	0.64	527.32
Jhelum	828.06	1488.00	713.68	2.96	0.44	0.44	658.59
Chenab	985.45	1374.61	682.65	1.53	0.28	0.28	398.03

Note: These data provide a numerical foundation for the Budyko distributions and ω estimates shown in Figure 4.

minor ($I_s < 0.2$), suggesting minimal hydroclimatic changes in the near term under a regime of restrictions on further greenhouse gas emissions. Under RCP8.5 (Figure 5c,d), more pronounced shifts were evident, especially in the Chenab and Jhelum basins, where I_s values ranged between 0.3 and 0.4, and θ_s indicated a stronger influence of PET. A north-northeastward shift was also observed in the Kabul and UIB basins, suggesting increased aridity driven by an increased atmospheric evaporative demand (PET) and moderate increases in precipitation (Wang et al. 2022). The distribution of arrows shows a steady movement towards higher aridity and increased evaporative demand across the sub-basins, highlighting the combined effects of increased precipitation and higher PET. In the mid-elevation basins, such as Kabul and Jhelum, this trend is accompanied by slight increases in rainfall, whereas in the Upper Indus Basin, the change is mainly driven by increasing atmospheric evaporative demand (PET), rather than by changes in precipitation.

Figure 6 illustrates wind rose plots, which depict the directional distribution of typical Budyko shifts (θ_rep) for each RCP scenario and time period (S: 2021–2040 and L: 2081–2100). Each segment of the plot represents the percentage of CORDEX models predicting a shift within that directional range, whereas the colour scale indicates the average shift magnitude (I_s) within the segment. In all panels, the primary shift direction is in the northeast quadrant (0°–90°), signifying concurrent increases in both aridity ($\varphi = \text{PET/P}$) and the evaporative index ($\varepsilon = \text{AET/P}$). Under the RCP8.5-L scenario (Figure 6d), shifts are the most frequent and significant, indicating stronger warming and an increase in PET. The concentration of bars in the 0°–45° sector highlights consistent responses across basins, particularly in long-term forecasts. These angular distributions indicate a consistent shift towards increasing aridity (stronger water limitation relative to atmospheric demand), driven by increasing atmospheric evaporative demand and rising aridity. The directional trends correspond with the spatial vectors depicted in Figure 5, where the sub-basins show similar northeastward trends. Consistent angular clustering also demonstrated the reliability of the modelled hydrological responses to climate change, despite variations among the models.

Table 2 provides a summary of the ensemble-based Budyko shift diagnostics for each sub-basin under the RCP4.5 and RCP8.5 scenarios during the near-term (2021–2040) and late-century (2081–2100) periods. The metrics include the Majority Quadrant (MQ), which identifies the most frequent quadrant of shift directions across the six CORDEX-RegCM4-4 simulations, with a value of 1 indicating that all shifts occurred within the same quadrant. MS (Majority Share) represents the percentage of

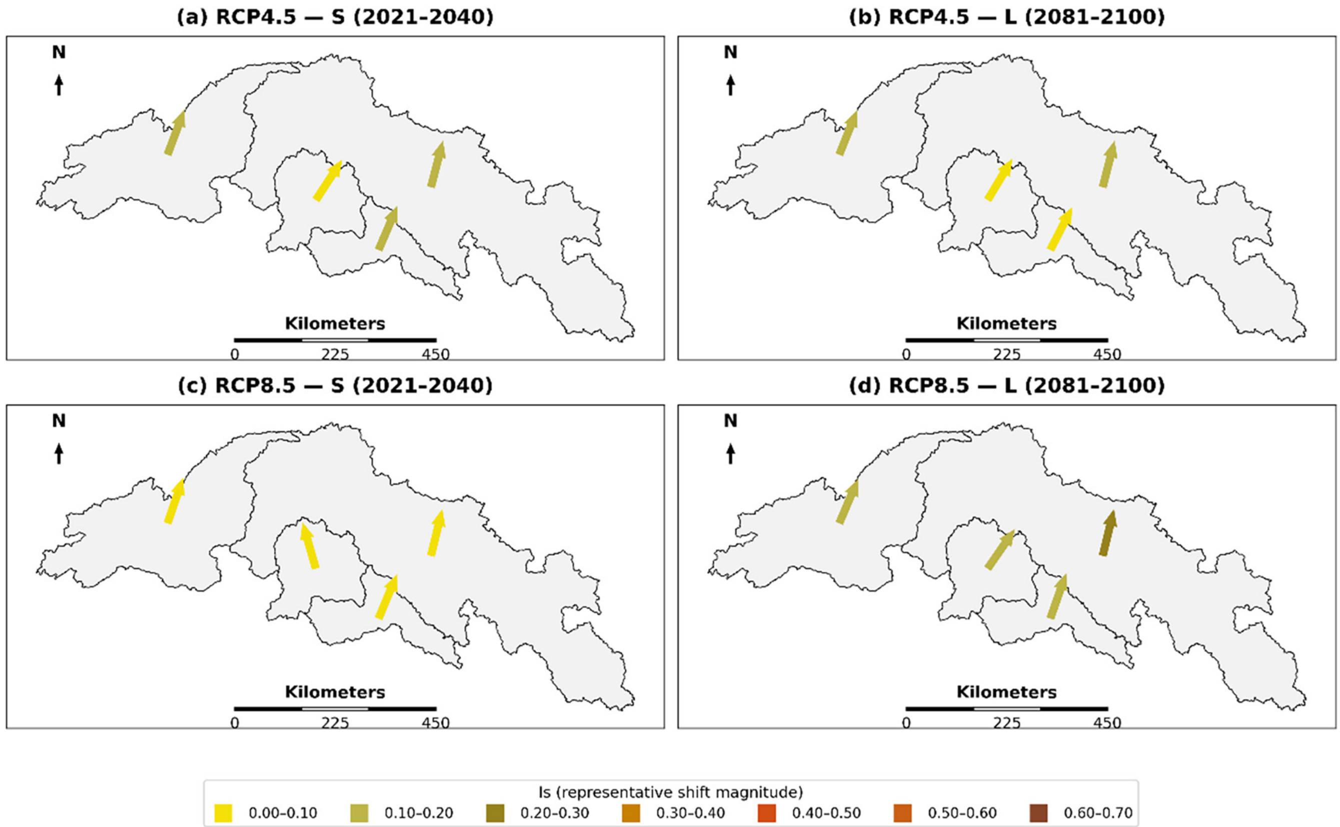

FIGURE 5 | (a–d) Representative Budyko shifts (I_s magnitude and θ_s direction) under RCP4.5 and RCP8.5 in the short- and long-term futures. Panels (a–d) correspond to (a) RCP4.5-S, (b) RCP4.5-L, (c) RCP8.5-S, and (d) RCP8.5-L. The arrows represent the direction of the Budyko space, and the color indicates the magnitude (I_s) of the hydroclimatic shift. [Colour figure can be viewed at wileyonlinelibrary.com]

ensemble members that fall into the majority quadrant. Shifts denote the number of models that contribute to the majority. Is_rep (Representative Shift Magnitude) measures the length of the ensemble mean shift vector in Budyko space, indicating the intensity of hydroclimatic changes. Θ_rep (Representative Angle) is the directional angle (in degrees) of the mean shift vector, measured counterclockwise from the east (aridity axis), showing the relative influence of precipitation versus evaporative demand. R_rep (Resultant Length) assesses ensemble coherence, where values near 1 suggest a high directional agreement among the models. Across all sub-basins, MQ consistently equals 1, indicating uniform shift directionality among the ensemble members. MS values range from 50% to 100%, and the number of contributing models varies from 3 to 6. The shift magnitudes (Is_rep) range from 0.005 to 0.20, with the largest shifts observed in the Kabul and Jhelum basins under the RCP8.5 scenario. These patterns indicate intensified hydroclimatic transitions in the catchments. Directional angles (θ_rep) range from 14° to 35°, generally indicating northeastward shifts in Budyko space, reflecting concurrent increases in both precipitation and PET, with the increase in PET generally dominating, leading to enhanced aridity. High R_rep values (≥0.99) across all cases reflect excellent inter-model consistency and robust ensemble means.

Figure 7 depicts the variation among models in terms of changes in hydroclimatic components, including changes in precipitation (ΔP), potential evapotranspiration (ΔPET), actual evapotranspiration (ΔAET), aridity index ($\Delta\varphi = \Delta(\text{PET/P})$), and evaporative index ($\Delta\varepsilon = \Delta(\text{AET/P})$) across the four sub-basins under the RCP4.5 and RCP8.5 scenarios. The boxes indicate the median and interquartile range from six CORDEX-RegCM4-4 simulations for both the near-future (S = 2021–2040, orange) and long-term (L = 2081–2100, green) periods. In the RCP4.5 scenario (Figure 7a), most basins experienced slight increases in both precipitation and PET, with ΔP showing strong spatial and inter-model variability, and ΔPET was consistently positive across the basins. The Jhelum and UIB basins consistently showed positive ΔAET, indicating improved moisture availability, whereas the Chenab Basin exhibited a wider range of model predictions and a short-term median ΔAET close to zero. These changes were more pronounced under RCP8.5 (Figure 7b); ΔP, ΔPET, and ΔAET all increased, particularly in the Jhelum and UIB basins. The $\Delta\varphi$ and $\Delta\varepsilon$ values indicate that aridity variations are becoming more severe with increasing forcing, primarily because of the rising PET. Even though there are positive trends in ΔAET, the wide range of inter-model variability emphasises the current uncertainty for the Chenab and Kabul rivers. The findings suggest that the primary factor influencing future hydroclimatic changes in the Indus sub-basins is a significant increase in potential evapotranspiration, with precipitation changes playing a less consistent and secondary role in this regard. While precipitation changes remain more varied between basins and models, rising atmospheric evaporative demand and increasing aridity are the key drivers of the expected Budyko shifts under RCP8.5.

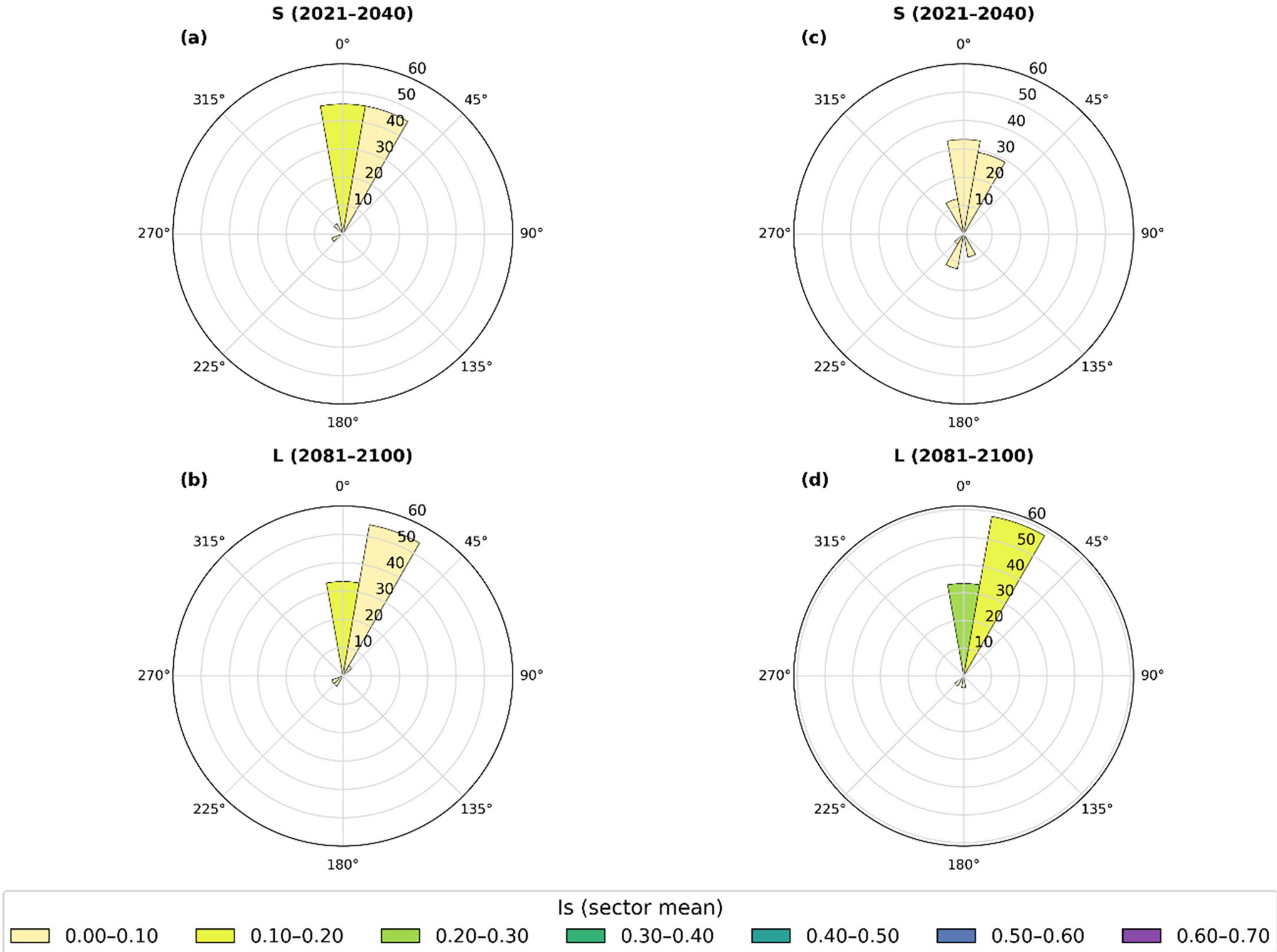

FIGURE 6 | (a–d) Wind-rose diagrams of Budyko shift directions (θ_s) under RCP4.5 and RCP8.5 scenarios. Panels (a, b) show near- and long-term futures (S = 2021–2040; L = 2081–2100) for RCP4.5, and panels (c d) for RCP8.5. The colour shading represents the sector mean. [Colour figure can be viewed at wileyonlinelibrary.com]

Figure 8 depicts the hydroclimatic factors influencing Budyko shifts within the Indus sub-basins by linking variations in the aridity index ($\Delta\varphi = \Delta(\text{PET/P})$) to variations in the evaporative ratio ($\Delta\varepsilon = \Delta(\text{AET/P})$). The four panels represent two emission scenarios (RCP4.5 and RCP8.5) and two future timeframes: near future (2021–2040) and late 21st century (2081–2100). Grey symbols indicate individual climate model outcomes, whereas coloured stars indicate basin-mean responses, highlighting the representative shift direction for each sub-basin. In every sub-basin and scenario, the anticipated Budyko shifts were marked by a positive $\Delta\varphi$, indicating an increase in atmospheric evaporative demand compared to precipitation. The corresponding $\Delta\varepsilon$ responses revealed basin-specific changes in the division of available water between evapotranspiration and runoff. It is important to recognise that these anticipated changes are not limited to a single Budyko curve trajectory. Instead, Δ(AET/P) signifies variations in evaporative efficiency influenced by both precipitation availability and atmospheric demand. This allows AET/P to decline even when PET/P increases. Under the RCP4.5 scenario, the short-term changes were generally mild, with the average basin responses concentrated near the center of the $\Delta\varphi$-$\Delta\varepsilon$ space, indicating minimal alterations in the hydroclimatic influence. By the end of the century, the average values for the basins move towards higher $\Delta\varphi$ and $\Delta\varepsilon$, particularly in the Jhelum and Upper Indus Basin. Under RCP8.5, there was a notable increase in the scale and variability of the model projections. The average shifts across basins moved farther into the upper-right section of the $\Delta\varphi - \Delta\varepsilon$ space, indicating more pronounced increases in aridity and a heightened evaporative response, particularly towards the end of the century.

5 | Discussion

5.1 | Factors Influencing Historical and Future Budyko Dynamics in the Indus Sub-Basins

Under the RCP4.5 and RCP8.5 scenarios, projections revealed consistent changes in the distribution of water and energy across all Indus sub-basins. The combined analysis of $\Delta\varphi$ and $\Delta\varepsilon$ suggests that future Budyko shifts are primarily driven by an increase in potential evapotranspiration. $\Delta\varphi$ consistently pointed northeastward (14°–35°) across all sub-basins, indicating a stronger influence of evaporative demand relative to precipitation changes. Increasing air temperatures increase the atmospheric demand for evapotranspiration, gradually

TABLE 2 | Summary of Budyko shift metrics for the four Indus sub-basins under RCP4.5 and RCP8.5 scenarios during the near-term (2021–2040) and late-century (2081–2100) periods, based on six CORDEX-RegCM4-4 simulations.

Basin	RCP	Period	MQ	MS	Shifts	Is_rep	Θ_rep	R_rep
Chenab	4.5	L	1	100	6	0.081	27.1	0.99
Jhelum	4.5	L	1	83.3	5	0.065	31	0.99
Kabul	4.5	L	1	83.3	5	0.107	21.8	1
UIB	4.5	L	1	100	6	0.101	14.4	1
Chenab	4.5	S	1	100	6	0.102	23.2	1
Jhelum	4.5	S	1	83.3	5	0.081	33.2	1
Kabul	4.5	S	1	83.3	5	0.107	20.5	1
UIB	4.5	S	1	100	6	0.106	14.5	1
Chenab	8.5	L	1	83.3	5	0.175	19.3	1
Jhelum	8.5	L	1	83.3	5	0.124	34.6	1
Kabul	8.5	L	1	100	6	0.18	23	1
UIB	8.5	L	1	100	6	0.2	13.6	1
Chenab	8.5	S	1	66.7	4	0.073	22.5	1
Jhelum	8.5	S	4	50	3	0.005	344	1
Kabul	8.5	S	1	66.7	4	0.051	18.9	1
UIB	8.5	S	1	83.3	5	0.063	13.7	1

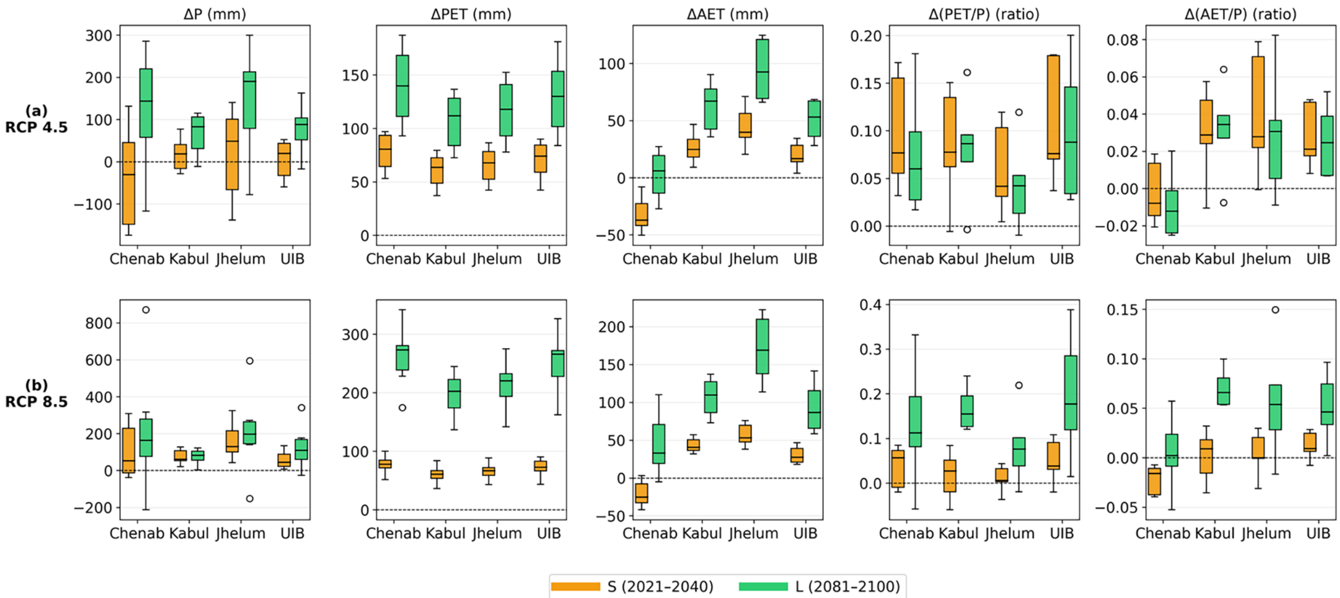

FIGURE 7 | (a, b) Changes in precipitation (ΔP), potential evapotranspiration (ΔPET), actual evapotranspiration (ΔAET), and derived indices across models for each sub basin under the RCP4.5 and RCP8.5 scenarios. [Colour figure can be viewed at wileyonlinelibrary.com]

pushing basins towards conditions with more limited water availability, especially in high-emission scenarios. This shift, primarily driven by increases in potential evapotranspiration, is consistent with the Budyko framework. This framework suggests that under warming conditions, long-term water balance is increasingly influenced by atmospheric energy supply rather than precipitation inputs (Greve et al. 2020; Saha et al. 2020). Similar patterns have been observed and predicted for the Indus Basin, where increased warming, earlier snowmelt, and changes in seasonal runoff patterns have been noted under the ongoing climate change (Wang et al. 2022; Ougahi and Mahmood 2022; Ali et al. 2023). Within the Budyko framework, these processes result in a systematic increase in evaporative partitioning, underscoring the significant role of atmospheric demand in shaping future hydroclimatic pathways.

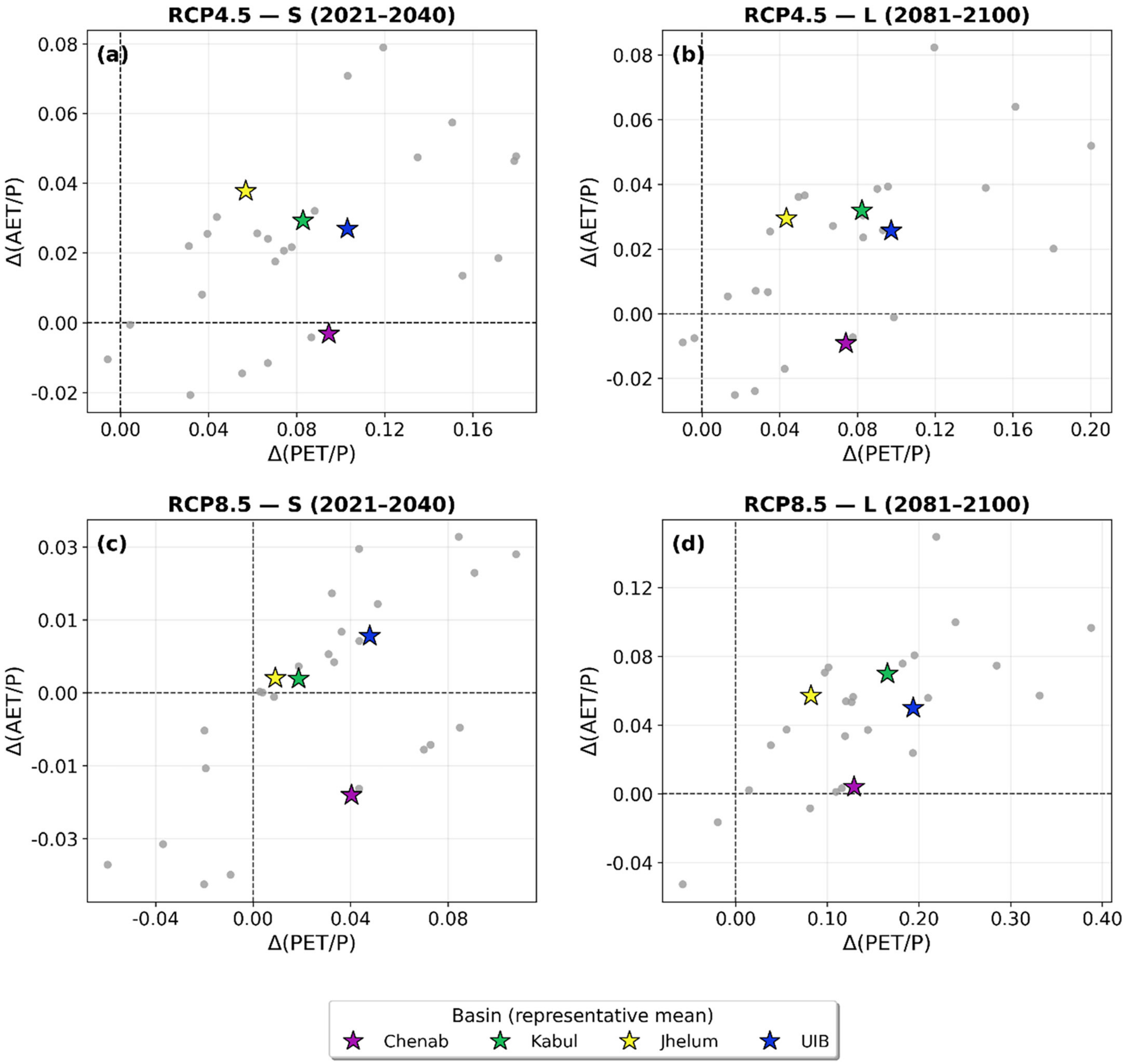

FIGURE 8 | (a–d) Scatter plots illustrating the hydroclimatic factors causing Budyko shifts across Indus sub-basins under both scenarios. Grey dots signify individual projections from the CORDEX RegCM4-4 model, whereas coloured stars represent the average responses for each basin. Dashed lines indicate no change in Δ(PET/P) and Δ(AET/P). Variations in AET/P demonstrate the combined water-energy balance responses, which may decline even if PET/P increases owing to diminished water availability in warmer conditions. [Colour figure can be viewed at wileyonlinelibrary.com]

The Budyko framework is applied here to multi-decadal mean conditions, where it has been demonstrated to provide a robust first-order description of long-term water–energy partitioning across diverse and heterogeneous catchments, including those affected by snow processes, even though the Upper Indus Basin is impacted by snow and glacier storage that introduces delayed meltwater contributions (Trancoso et al. 2016; Gnann et al. 2019; Berghuijs et al. 2020). The long-term Budyko closure assumption is not violated in this situation because cryospheric storage is understood as a seasonal redistribution mechanism rather than a stable long-term storage component.

It is crucial to note that snow and glacier storage mechanisms are not specifically represented in the Budyko framework (Equation 7). Rather, seasonal storage and delayed melt contributions are implicitly included in the multi-decadal water balance by applying long-term mean values of precipitation, potential evapotranspiration, and runoff. According to this hypothesis, the calibrated ω parameter and the observed P–Q relationship reflect the combined effects of cryospheric processes, which mainly affect runoff timing rather than the long-term partitioning between water and energy (Trancoso et al. 2016; Gnann et al. 2019; Berghuijs et al. 2020; Lee et al. 2023).

Although there is a commonality, the extent of the Budyko shifts differs significantly across the sub-basins, highlighting the strong influence of elevation and cryospheric factors. The northeastward orientation of the ensemble mean shift vectors across most basins suggests simultaneous increases in PET and P, with a more pronounced influence of evaporative demand. This aligns with the energy-dominated responses anticipated in warming scenarios. The Budyko shifts in the Upper Indus and Chenab Basins were relatively moderate compared to those in lower-elevation basins, which may indicate the buffering effect of cryospheric storage. In these regions, a large portion of runoff originates from the delayed release of meltwater from seasonal snowpacks and glaciers, which disconnects streamflow generation from current precipitation and atmospheric evaporative demands. Observational and modelling studies in the Upper Indus have shown that precipitation gradients controlled by elevation, winter westerly disturbances, and ongoing glacier storage reduce the immediate hydrological sensitivity to warming (Immerzeel et al. 2015; Dahri et al. 2018; Shafeeque and Luo 2021). This cryospheric buffering effect has also been found to stabilise annual runoff despite increasing PET, particularly in catchments fed by snow and glaciers (Yaseen et al. 2022; Ougahi and Mahmood 2022).

Conversely, the Kabul and Jhelum basins exhibited more pronounced and consistent transitions towards water-limited conditions. This may be attributed to their lower altitudes, reduced cryospheric impact, and greater reliance on monsoonal precipitation. In these regions, runoff is more directly influenced by the rising atmospheric evaporative demand (PET), leading to increased actual evapotranspiration losses and reduces runoff efficiency. The uniform positive directional angles observed in all basins suggest northeastward Budyko shifts, characterised by increases in both precipitation and PET values. However, PET predominates, emphasising energy-driven and hydroclimatic responses. Previous hydroclimatic studies on monsoon-affected Indus sub-basins have reported that warming leads to higher evapotranspiration, shifts in precipitation patterns, and reduced summer runoff efficiency, particularly under high-emission scenarios (Yaseen et al. 2022; Wang et al. 2022; Ougahi and Mahmood 2022). These basins, which are sensitive to energy changes, underwent significant changes in evaporation rates, along with basin-specific increases in dryness, leading to more pronounced Budyko shifts than those at higher altitudes.

5.2 | Effects of Budyko Alterations on Water Resources and Variability

Multi-model ensemble analysis indicated a significant increase in uncertainty under RCP8.5, as evidenced by a wider range of both the extent and direction of Budyko shifts. This increased variability underscores the heightened sensitivity of basin-scale hydrological responses to radiative forcing in high-emission scenarios owing to the compounded uncertainties in temperature amplification, PET estimation, and precipitation representation in complex mountainous regions. Previous evaluations of CORDEX South Asia simulations have highlighted considerable inter-model variability in the depiction of orographic precipitation and surface energy balance processes over the Indus headwaters, leading to divergent hydrological outcomes under intense warming conditions (Giorgi et al. 2009; Shafeeque and Luo 2021). Recent evaluations have also underscored rising temperatures, increased precipitation variability, and the intensification of extreme rainfall events throughout the Indus Basin, all of which contribute to heightened hydroclimatic uncertainty on a regional scale (Heureux et al. 2022). In this scenario, the Budyko framework serves as a physically consistent diagnostic tool for interpreting ensemble uncertainty by directly linking it to changes in the water supply and atmospheric demand. Table S2 summarises the findings of a further evaluation of the projected AET's sensitivity to the stationary-ω assumption using $\pm 10\%$ perturbations of the calibrated ω.

In summary, these results indicate that long-term alterations in the water balance of the Indus Basin are influenced by the interplay of rising atmospheric evaporative demand, elevation-dependent cryospheric buffering, basin-specific climatic factors, and precipitation patterns. The Budyko framework can help identify the likely effects of these mechanisms on water budgets in high-altitude regions with limited data, illustrating how drying driven by potential evapotranspiration (PET), temporary meltwater buffering, and increasing model uncertainty collectively affects future water availability in these regions. These findings highlight the importance of developing adaptive water management strategies that explicitly account for changing melt dynamics, increased evaporative demand, and greater uncertainty under high-emission scenarios, particularly in Indus sub-basins with varying elevations and climatic conditions. From the perspective of water resources, the anticipated increase in dryness and evaporative demand suggests an increasing strain on runoff generation at the basin level, with significant consequences for water availability throughout the seasons. These changes in hydroclimatic conditions present distinct challenges for water management. The rise in evaporative demand leads to increased water loss from reservoirs and irrigation systems, indicating a need for better storage solutions and more efficient water use (Laghari et al. 2012). In basins fed by snow and glaciers, the earlier melting and seasonal changes in runoff underscore the necessity for adaptive reservoir management to handle the changing water supply (Archer and Fowler 2004; Tahir et al. 2011; Ali et al. 2023). In areas downstream, the decrease in effective water availability might require shifts in crop selection towards varieties that use less water and the implementation of more efficient irrigation methods (Laghari et al. 2012). Additionally, given the transboundary nature of the Indus River system, these alterations could further strain existing water-sharing agreements, underscoring the importance of flexible, co-operative basin-level management strategies (Miner et al. 2009). Basins at lower elevations and those influenced by monsoons are expected to be more susceptible to climate-induced water stress, whereas high-altitude basins may encounter delayed but possibly sudden changes as the buffering capacity of the cryosphere diminishes.

In this study, we utilised a modified Budyko framework to assess long-term hydroclimatic patterns for major sub-basins of the Indus River. This study focused on the average distribution of water and energy without specifically addressing seasonal variations or short-term hydrological extremes in the region. Additionally, for high-altitude basins, the impact of cryospheric elements on runoff is understood through basin-wide responses rather than through detailed simulations of snow accumulation, glacier mass balance, or melting.

Moreover, potential evapotranspiration serves as a comprehensive measure of atmospheric energy demand, enabling uniform comparisons across basins and scenarios. However, it does not address the detailed surface energy balance processes or the extreme heat events. Ultimately, the conclusions aim to describe hydroclimatic responses at the basin scale and their relative sensitivities, rather than focusing on local hydrological impacts. Future research incorporating seasonal Budyko diagnostics, detailed cryospheric modeling, and more granular analyses will enhance our understanding of water availability and timing in the context of ongoing climate change.

While the basin-scale patterns identified in this study are robust across climate models, it is important to recognise several limitations. The analysis was performed on an annual basis using the Budyko framework, which does not specifically address seasonal hydroclimatic variations or extreme events that are crucial for water management. Additionally, cryospheric influences were indirectly represented through long-term water–energy partitioning rather than through direct modelling of snow accumulation, glacier mass balance, and melt dynamics, which can affect short-term runoff responses in high-altitude basins. There are also uncertainties in the representation of potential evapotranspiration, especially in areas with complex topography and climate conditions. Therefore, future research should incorporate seasonal diagnostics, better representation of cryospheric processes, and more accurate estimates of evaporative demand within integrated climate–hydrology frameworks to better define basin-specific sensitivities and improve the predictability of hydroclimatic responses under continued warming.

Although the wider Indus River system is strongly influenced by human interventions, including reservoirs, diversions, irrigation return flows, and groundwater abstraction, the gauging stations used in this study are located upstream of major reservoir control structures (Ali et al. 2023), which reduces the influence of large-scale flow regulation on the observed discharge. Accordingly, Budyko analysis is interpreted primarily as representing hydroclimate-dominated water–energy partitioning in the upstream study catchments rather than the fully managed downstream hydrology of the Indus irrigation system. The Lower Indus Basin is distinguished by a vast network of hydraulic structures linked to the Indus Basin Irrigation System (IBIS), such as barrages, canals, and diversions, which significantly alter the natural flow patterns and shape of the river. As a result, the hydrology downstream is heavily controlled and somewhat disconnected from direct climatic influences, reducing the effectiveness of Budyko-type analysis in these areas (Fatima et al. 2025). Nevertheless, residual anthropogenic influences cannot be completely excluded and may introduce some uncertainty into runoff and the inferred evapotranspiration and Budyko indices. Therefore, the results are interpreted as reflecting hydroclimatic responses under limited anthropogenic influence rather than fully managed hydrological conditions.

6 | Conclusion

This study applied the Budyko framework to investigate the past hydroclimatic conditions and future distribution of water and energy in the Upper Indus, Kabul, Jhelum, and Chenab sub-basins. The initial analysis highlighted significant spatial variability in hydroclimatic patterns. Basins at higher altitudes exhibited lower evapotranspiration rates and a greater emphasis on runoff, whereas those at mid-to-lower elevations were more responsive to atmospheric evaporative demand, underscoring the importance of physiographic factors in shaping long-term water balance dynamics.

Projections for the future under RCP4.5 and RCP8.5 indicate drier hydroclimatic conditions in most sub-basins, with increased aridity primarily caused by rising potential evapotranspiration rather than offsetting precipitation increases. Although cryospheric buffering tempers short-term responses in high-altitude basins, these areas may experience delayed, yet potentially sudden, hydrological shifts as temperatures continue to rise. In contrast, basins at lower elevations and those influenced by monsoons showed a more immediate reaction to increased evaporative demand, resulting in greater susceptibility to future water stress, especially under high-emission scenarios.

Overall, the results underscore the significant influence of atmospheric energy demand on future water availability at the basin scale in the Indus Basin, while also highlighting the increasing uncertainty of hydroclimatic responses owing to intensified warming. Employing a multi-model ensemble within the Budyko framework offers a physically coherent and data-efficient method for assessing hydroclimatic sensitivity in complex mountain regions with limited data. This framework provides crucial insights into long-term water resource management and climate adaptation strategies in river basins affected by glaciers and monsoons, which are experiencing increasing climatic uncertainty. Future work will extend this analysis using CMIP6/SSP-based dynamically downscaled regional climate simulations for South Asia.

Author Contributions

Chia-Jeng Chen: conceptualization, methodology, validation, investigation, resources, writing – original draft, supervision, project administration, funding acquisition. **Muhammad Arif:** data curation, formal analysis, visualization, writing – original draft. **Tsung-Yu Lee:** conceptualization, methodology, writing – review and editing. **Nir Krakauer:** writing – review and editing, supervision.

Acknowledgements

The authors acknowledge Ali et al. (2023) for making the streamflow data publicly available, which supported the hydrological analysis conducted in this study.

Funding

This study is partially supported by Taiwan's National Science and Technology Council (NSTC 114-2628-E-005-003-MY3).

Conflicts of Interest

The authors declare no conflicts of interest.

Data Availability Statement

The datasets used and/or analysed during the current study are available from the corresponding author (cjchen@nchu.edu.tw) upon reasonable requests.

References

Ahmed, K., S. Shahid, X. Wang, N. Nawaz, and N. Khan. 2019. "Spatiotemporal Changes in Aridity of Pakistan During 1901–2016." *Hydrology and Earth System Sciences* 23, no. 7: 3081–3096.

Ali, S., B.-H. Kim, T. Akhtar, and J. Kam. 2023. "Past and Future Changes Toward Earlier Timing of Streamflow Over Pakistan From Bias-Corrected Regional Climate Projections (1962–2099)." *Journal of Hydrology* 617: 128959.

Archer, D. R., and H. J. Fowler. 2004. "Spatial and Temporal Variations in Precipitation in the Upper Indus Basin, Global Teleconnections and Hydrological Implications." *Hydrology and Earth System Sciences* 8, no. 1: 47–61.

Aschonitis, V., D. Touloumidis, M. C. ten Veldhuis, and M. Coenders-Gerrits. 2022. "Correcting Thornthwaite Potential Evapotranspiration Using a Global Grid of Local Coefficients to Support Temperature-Based Estimations of Reference Evapotranspiration and Aridity Indices." *Earth System Science Data* 14, no. 1: 163–177.

Asghar, A., J. Iqbal, A. Amin, and L. Ribbe. 2019. "Integrated Hydrological Modeling for Assessment of Water Demand and Supply Under Socio-Economic and IPCC Climate Change Scenarios Using WEAP in Central Indus Basin." *Journal of Water Supply Research and Technology-AQUA* 68, no. 2: 136–148.

Atif, S., M. Umar, and F. Ullah. 2021. "Investigating the Flood Damages in Lower Indus Basin Since 2000: Spatiotemporal Analyses of the Major Flood Events." *Natural Hazards* 108, no. 2: 2357–2383.

Berghuijs, W. R., S. J. Gnann, and R. A. Woods. 2020. "Unanswered Questions on the Budyko Framework." *Journal of Hydrology* 265, no. 26: 164–177.

Berghuijs, W. R., J. R. Larsen, T. H. van Emmerik, and R. A. Woods. 2017. "A Global Assessment of Runoff Sensitivity to Changes in Precipitation, Potential Evaporation, and Other Factors." *Water Resources Research* 53, no. 10: 8475–8486.

Cannon, A. J., S. R. Sobie, and T. Q. Murdock. 2015. "Bias Correction of GCM Precipitation by Quantile Mapping: How Well Do Methods Preserve Changes in Quantiles and Extremes?" *Journal of Climate* 28, no. 17: 6938–6959.

Cannon, F., L. M. Carvalho, C. Jones, and J. Norris. 2016. "Winter Westerly Disturbance Dynamics and Precipitation in the Western Himalaya and Karakoram: A Wave-Tracking Approach." *Theoretical and Applied Climatology* 125, no. 1: 27–44.

Chatterjee, R. 2024. "Overview of Climate Change Data on India and SAARC Countries." *Journal of Earth System Science* 133, no. 4: 198.

Chen, J., Y. Yang, and J. Tang. 2022. "Bias Correction of Surface Air Temperature and Precipitation in CORDEX East Asia Simulation: What Should We Do When Applying Bias Correction?" *Atmospheric Research* 280: 106439.

Choudhary, A., and A. P. Dimri. 2018. "Assessment of CORDEX-South Asia Experiments for Monsoonal Precipitation Over Himalayan Region for Future Climate." *Climate Dynamics* 50, no. 7: 3009–3030.

Dahri, Z. H., F. Ludwig, E. Moors, et al. 2021. "Climate Change and Hydrological Regime of the High-Altitude Indus Basin Under Extreme Climate Scenarios." *Science of the Total Environment* 768: 144467.

Dahri, Z. H., E. Moors, F. Ludwig, et al. 2018. "Adjustment of Measurement Errors to Reconcile Precipitation Distribution in the High-Altitude Indus Basin." *International Journal of Climatology* 38, no. 10: 3842–3860.

Dallaire, G., A. Poulin, R. Arsenault, and F. Brissette. 2021. "Uncertainty of Potential Evapotranspiration Modelling in Climate Change Impact Studies on Low Flows in North America." *Hydrological Sciences Journal* 66, no. 4: 689–702.

Demeke, G. G., J.-C. Huang, and Y.-Y. Chen. 2025. "Runoff Generation Signaled by Deviations From the Budyko Framework." *Water Resources Management* 39, no. 5: 2133–2148.

Dimri, A. P., D. Kumar, S. Chopra, and A. Choudhary. 2019. "Indus River Basin: Future Climate and Water Budget." *International Journal of Climatology* 39, no. 1: 395–406.

Dubey, A., D. Swami, V. Gupta, and N. Joshi. 2023. "From the Peaks to the Plains: Investigating the Role of Elevation in Governing Drought Dynamics Over the Indus River Basin." *Atmospheric Research* 291: 106824.

Fatima, R., S. Atif, M. Fort, and M. Azmat. 2025. "Channel Morphology of the Indus, and the Growing Risk of Floods Related Damages in the Indus River Basin." *Natural Hazards* 121, no. 13: 15789–15821.

Feng, J., Y. Alifujiang, S. Kozhokulov, Y. Jiang, and P. Yang. 2025. "Quantifying Hydrological Sensitivity in Central Asia: A Multi-Factor Budyko Framework Analysis (2000–2020)." *Journal of Hydrology: Regional Studies* 61: 102746.

Fu, B. P. 1981. "On the Calculation of the Evaporation From Land Surface." *Scientia Atmospherica Sinica* 5: 23–31.

Giese, A., S. Rupper, D. Keeler, E. Johnson, and R. Forster. 2022. "Indus River Basin Glacier Melt at the Subbasin Scale." *Frontiers in Earth Science* 10: 767411.

Giorgi, F., C. Jones, and G. R. Asrar. 2009. "Addressing Climate Information Needs at the Regional Level: The CORDEX Framework." *World Meteorological Organization (WMO) Bulletin* 58, no. 3: 175.

Gnann, S. J., R. A. Woods, and N. J. Howden. 2019. "Is There a Baseflow Budyko Curve?" *Water Resources Research* 55, no. 4: 2838–2855.

Greve, P., P. Burek, and Y. Wada. 2020. "Using the Budyko Framework for Calibrating a Global Hydrological Model." *Water Resources Research* 56, no. 6: e2019WR026280.

Gudmundsson, L., J. B. Bremnes, J. E. Haugen, and T. Engen-Skaugen. 2012. "Downscaling RCM Precipitation to the Station Scale Using Statistical Transformations—A Comparison of Methods." *Hydrology and Earth System Sciences* 16: 3383–3390.

Harris, I., T. Osborn, P. Jones, and D. Lister. 2020. "Version 4 of the CRU TS Monthly High-Resolution Gridded Multivariate Climate Dataset." *Scientific Data* 7: 109.

Heureux, A. M. C., J. Alvar-Beltrán, R. Manzanas, et al. 2022. "Climate Trends and Extremes in the Indus River Basin, Pakistan: Implications for Agricultural Production." *Atmosphere* 13, no. 3: 378.

Holthuijzen, M., B. Beckage, P. J. Clemins, D. Higdon, and J. M. Winter. 2022. "Robust Bias-Correction of Precipitation Extremes Using a Novel Hybrid Empirical Quantile-Mapping Method: Advantages of a Linear Correction for Extremes." *Theoretical and Applied Climatology* 149, no. 1: 863–882.

Hussain, A., J. Cao, S. Ali, et al. 2022. "Variability in Runoff and Responses to Land and Oceanic Parameters in the Source Region of the Indus River." *Ecological Indicators* 140: 109014.

Hussain, A., I. Hussain, S. Ali, et al. 2023. "Assessment of Precipitation Extremes and Their Association With NDVI, Monsoon and Oceanic Indices Over Pakistan." *Atmospheric Research* 292: 106873.

Immerzeel, W. W., N. Wanders, A. F. Lutz, J. M. Shea, and M. F. P. Bierkens. 2015. "Reconciling High-Altitude Precipitation in the Upper

Indus Basin With Glacier Mass Balances and Runoff." *Hydrology and Earth System Sciences* 19, no. 11: 4673–4687.

Iqbal, W., F. Syed, H. Sajjad, G. Nikulin, E. Kjellström, and A. Hannachi. 2017. "Mean Climate and Representation of Jet Streams in the CORDEX South Asia Simulations by the Regional Climate Model RCA4." *Theoretical and Applied Climatology* 129, no. 1: 1–19.

Jamshed, R., E. Naeem, A. A. Tahir, et al. 2025. "Modeling Snowmelt-Driven Streamflow Dynamics in a Himalayan Basin Under Climate Warming Scenarios." *PLOS Climate* 4, no. 10: e0000739.

Kan, B., F. Su, B. Xu, Y. Xie, J. Li, and H. Zhang. 2018. "Generation of High Mountain Precipitation and Temperature Data for a Quantitative Assessment of Flow Regime in the Upper Yarkant Basin in the Karakoram." *Journal of Geophysical Research: Atmospheres* 123, no. 16: 8462–8486.

Khan, S. I., and T. E. Adams, eds. 2019. *Indus River Basin: Water Security and Sustainability*. Elsevier.

Koppa, A., and M. Gebremichael. 2017. "A Framework for Validation of Remotely Sensed Precipitation and Evapotranspiration Based on the Budyko Hypothesis." *Water Resources Research* 53, no. 10: 8487–8499.

Kotamarthi, R., K. Hayhoe, D. Wuebbles, L. O. Mearns, J. Jacobs, and J. Jurado. 2021. *Downscaling Techniques for High-Resolution Climate Projections: From Global Change to Local Impacts*. Cambridge University Press.

Krakauer, N. Y., T. Lakhankar, and G. H. Dars. 2019. "Precipitation Trends Over the Indus Basin." *Climate* 7, no. 10: 116.

Kumar, D., and A. Dimri. 2018. "Regional Climate Projections for Northeast India: An Appraisal From CORDEX South Asia Experiment." *Theoretical and Applied Climatology* 134, no. 3: 1065–1081.

Kuo, C.-M., Y.-Z. Chen, and S.-T. Chen. 2024. "Applying Budyko Framework to Explore the Projected Hydrologic Changes in Southern Taiwan." *Terrestrial, Atmospheric and Oceanic Sciences* 35, no. 1: 1–20.

Laghari, A. N., D. Vanham, and W. Rauch. 2012. "The Indus Basin in the Framework of Current and Future Water Resources Management." *Hydrology and Earth System Sciences* 16, no. 4: 1063–1083.

Latif, Y., Y. Ma, and W. Ma. 2021. "Climatic Trends Variability and Concerning Flow Regime of Upper Indus Basin, Jehlum, and Kabul River Basins Pakistan." *Theoretical and Applied Climatology* 144: 447–468.

Lee, T.-Y., Y.-C. Chen, S.-E. Chen, J.-Y. Lee, C.-C. Chiu, and C.-J. Chen. 2026. "Decoupling of Precipitation and Streamflow Trends Induced by Forest Expansion: Evidence From Time-Varying Budyko Analysis." *Journal of Hydrology: Regional Studies* 64: 103317.

Lee, T.-Y., C.-C. Chiu, C.-J. Chen, C.-Y. Lin, and F.-K. Shiah. 2023. "Assessing Future Availability of Water Resources in Taiwan Based on the Budyko Framework." *Ecological Indicators* 146: 109808.

Lehner, B., K. Verdin, and A. Jarvis. 2008. "New Global Hydrography Derived From Spaceborne Elevation Data." *Eos, Transactions American Geophysical Union* 89, no. 10: 93–94.

Li, D., M. Pan, Z. Cong, L. Zhang, and E. Wood. 2013. "Vegetation Control on Water and Energy Balance Within the Budyko Framework." *Water Resources Research* 49, no. 2: 969–976.

Li, Y., Y. Qin, and P. Rong. 2022. "Evolution of Potential Evapotranspiration and Its Sensitivity to Climate Change Based on the Thornthwaite, Hargreaves, and Penman–Monteith Equation in Environmental Sensitive Areas of China." *Atmospheric Research* 273: 106178.

Liaqat, M. U., G. Grossi, S. U. Hasson, and R. Ranzi. 2022. "Characterization of Interannual and Seasonal Variability of Hydro-Climatic Trends in the Upper Indus Basin." *Theoretical and Applied Climatology* 147, no. 3: 1163–1184.

Liu, X., and B. Chen. 2000. "Climatic Warming in the Tibetan Plateau During Recent Decades." *International Journal of Climatology: A Journal of the Royal Meteorological Society* 20, no. 14: 1729–1742.

Luo, H., Z. Wang, C. He, D. Chen, and S. Yang. 2024. "Future Changes in South Asian Summer Monsoon Circulation Under Global Warming: Role of the Tibetan Plateau Latent Heating." *NPJ Climate and Atmospheric Science* 7, no. 1: 103.

Maurer, T., F. Avanzi, S. D. Glaser, and R. C. Bales. 2022. "Drivers of Drought-Induced Shifts in the Water Balance Through a Budyko Approach." *Hydrology and Earth System Sciences* 26, no. 3: 589–607.

McSweeney, C. F., R. G. Jones, and B. B. Booth. 2012. "Selecting Ensemble Members to Provide Regional Climate Change Information." *Journal of Climate* 25, no. 20: 7100–7121.

Miner, M., G. Patankar, S. Gamkhar, and D. J. Eaton. 2009. "Water Sharing Between India and Pakistan: A Critical Evaluation of the Indus Water Treaty." *Water International* 34, no. 2: 204–216.

Mondal, S. K., H. Tao, J. Huang, et al. 2021. "Projected Changes in Temperature, Precipitation and Potential Evapotranspiration Across Indus River Basin at 1.5–3.0°C Warming Levels Using CMIP6-GCMs." *Science of the Total Environment* 789: 147867.

Mukhopadhyay, B., and A. Khan. 2015. "A Reevaluation of the Snowmelt and Glacial Melt in River Flows Within Upper Indus Basin and Its Significance in a Changing Climate." *Journal of Hydrology* 527: 119–132.

Munchak, S. J., R. Roy, and J. L'Heureux. 2022. "Use of Deep and Convolutional Neural Networks to Evaluate Spaceborne Radar, Sounder, and Geostationary Precipitation Retrievals." AGU Fall Meeting Abstracts.

Muzammil, M., A. Zahid, and L. Breuer. 2020. "Water Resources Management Strategies for Irrigated Agriculture in the Indus Basin of Pakistan." *Water* 12, no. 5: 1429.

Ngai, S. T., F. Tangang, and L. Juneng. 2017. "Bias Correction of Global and Regional Simulated Daily Precipitation and Surface Mean Temperature Over Southeast Asia Using Quantile Mapping Method." *Global and Planetary Change* 149: 79–90.

Oliveira-Aparecido, L. E., A. F. Dutra, P. A. Lorençone, F. de Alcântara Neto, J. A. Lorençon, and M. R. L. Leite. 2021. "Climate Change in MATOPIBA Region of Brazil Using Thornthwaite (1948) Classification." *Research Square*. https://www.researchsquare.com/article/rs-428799/v1.

Ougahi, J. H., and S. A. Mahmood. 2022. "Evaluation of Satellite-Based and Reanalysis Precipitation Datasets by Hydrologic Simulation in the Chenab River Basin." *Journal of Water and Climate Change* 13, no. 3: 1563–1582.

Qureshi, A. S., and C. Perry. 2021. "Managing Water and Salt for Sustainable Agriculture in the Indus Basin of Pakistan." *Sustainability* 13, no. 9: 5303.

Rajbhandari, R., A. Shrestha, A. Kulkarni, S. Patwardhan, and S. Bajracharya. 2015. "Projected Changes in Climate Over the Indus River Basin Using a High Resolution Regional Climate Model (PRECIS)." *Climate Dynamics* 44, no. 1: 339–357.

Rakhmatova, N., M. Arushanov, L. Shardakova, et al. 2021. "Evaluation of the Perspective of ERA-Interim and ERA5 Reanalyses for Calculation of Drought Indicators for Uzbekistan." *Atmosphere* 12, no. 5: 527.

Rao, K. K., T. V. L. Kumar, A. Kulkarni, J. S. Chowdary, and S. Desamsetti. 2022. "Characteristic Changes in Climate Projections Over Indus Basin Using the Bias Corrected CMIP6 Simulations." *Climate Dynamics* 58: 3471–3495.

Riley, C., S. Rupper, J. W. Steenburgh, C. Strong, A. K. Kochanski, and S. Wolvin. 2021. "Characteristics of Historical Precipitation in High Mountain Asia Based on a 15-Year High Resolution Dynamical Downscaling." *Atmosphere* 12, no. 3: 355.

Sa'adi, Z., M. S. Shiru, S. Shahid, and T. Ismail. 2020. "Selection of General Circulation Models for the Projections of Spatio-Temporal Changes in Temperature of Borneo Island Based on CMIP5." *Theoretical and Applied Climatology* 139: 351–371.

Saha, A., M. K. Jain, P. Joshi, S. Das, and N. S. Rawat. 2025. "Development of Daily Downscaled, Bias-Corrected CMIP6 Climate Datasets for Estimating Reference Evapotranspiration (ETo) in South Asia." *Scientific Data* 12: 1879.

Saha, A., J. Joseph, and S. Ghosh. 2020. "Climate Controls on the Terrestrial Water Balance: Influence of Aridity on the Basin Characteristics Parameter in the Budyko Framework." *Science of the Total Environment* 739: 139863.

Santos, C. N., A. A. R. Santos, M. C. Abreu, et al. 2024. "Monthly Potential Evapotranspiration Estimated Using the Thornthwaite Method With Gridded Climate Datasets in Southeastern Brazil." *Theoretical and Applied Climatology* 155, no. 5: 3739–3756.

Sarwar, J., S. A. Khan, M. Azmat, F. Khan, and S. Javed. 2026. "A GIS-Based Technique for Estimation of Economic Losses From Riverine Flood in the Lower Indus Basin." *Natural Hazards* 122, no. 1: 31.

Sattar, H., and T. Kinouchi. 2025. "Streamflow Estimation in the Indus River Basin Using a Water Balance Framework and Artificial Neural Networks With Satellite- and Model-Derived Global Hydro-Climatic Data Sources." *Journal of Hydrology: Regional Studies* 60: 102510.

Shafeeque, M., and Y. Luo. 2021. "A Multi-Perspective Approach for Selecting CMIP6 Scenarios to Project Climate Change Impacts on Glacio-Hydrology With a Case Study in Upper Indus River Basin." *Journal of Hydrology* 599: 126466.

Shafeeque, M., Y. Luo, and H. He. 2022. "Involving Turc-Budyko Formula in Evaluating Gridded Precipitation Datasets in Glaciated Catchments." *Journal of Hydrology* 614: 128482.

Shah, M., M. B. Huda, N. A. Rather, M. Lone, and S. Eslamian. 2024. "13 Global Regional Climate Climate Modeling Downscaling and." In *Handbook of Climate Change Impacts on River Basin Management: Fundamentals and Impacts*, 207. CRC Press.

Shaw, S. B., and S. J. Riha. 2011. "Assessing Temperature-Based PET Equations Under a Changing Climate in Temperate, Deciduous Forests." *Hydrological Processes* 25, no. 9: 1466–1478.

Siegfried, T., A. U. H. Mujahid, B. Marti, P. Molnar, D. N. Karger, and A. Yakovlev. 2024. "Unveiling the Future Water Pulse of Central Asia: A Comprehensive 21st Century Hydrological Forecast From Stochastic Water Balance Modeling." *Climatic Change* 177, no. 9: 141.

Sun, H., X. Wang, Y. Qu, J. Lyu, H. Cai, and X. Zhang. 2025. "Interpretation of the Budyko Framework for Monthly Evapotranspiration Prediction of Individual Basins." *Atmospheric Research* 315: 107895.

Tahir, A. A., P. Chevallier, Y. Arnaud, L. Neppel, and B. Ahmad. 2011. "Modeling Snowmelt-Runoff Under Climate Scenarios in the Hunza River Basin, Karakoram Range, Northern Pakistan." *Journal of Hydrology* 409, no. 1–2: 104–117.

Thompson, J. R., A. J. Green, and D. G. Kingston. 2014. "Potential Evapotranspiration-Related Uncertainty in Climate Change Impacts on River Flow: An Assessment for the Mekong River Basin." *Journal of Hydrology* 510: 259–279.

Thornthwaite, C. W. 1948. "An Approach Toward a Rational Classification of Climate." *Geographical Review* 38, no. 1: 55–94.

Tong, Y., X. Gao, Z. Han, Y. Xu, Y. Xu, and F. Giorgi. 2021. "Bias Correction of Temperature and Precipitation Over China for RCM Simulations Using the QM and QDM Methods." *Climate Dynamics* 57, no. 5: 1425–1443.

Trajkovic, S. 2005. "Temperature-Based Approaches for Estimating Reference Evapotranspiration." *Journal of Irrigation and Drainage Engineering* 131, no. 4: 316–323.

Trancoso, R., J. R. Larsen, C. McAlpine, T. R. McVicar, and S. Phinn. 2016. "Linking the Budyko Framework and the Dunne Diagram." *Journal of Hydrology* 535: 581–597.

Vremec, M., R. A. Collenteur, and S. Birk. 2024. "PyEt v1.3.1: A Python Package for the Estimation of Potential Evapotranspiration." *Geoscientific Model Development* 17, no. 18: 7083–7103.

Wang, C., S. Wang, B. Fu, and L. Zhang. 2016. "Advances in Hydrological Modelling With the Budyko Framework: A Review." *Progress in Physical Geography* 40, no. 3: 409–430.

Wang, D., and Y. Tang. 2014. "A One-Parameter Budyko Model for Water Balance Captures Emergent Behavior in Darwinian Hydrologic Models." *Geophysical Research Letters* 41, no. 13: 4569–4577.

Wang, L., X. Wang, J. Chang, et al. 2025. "Regional Water Supply Capacity Assessment in Different Drought Scenarios Based on Budyko Supply and Demand Framework." *Journal of Hydrology: Regional Studies* 62: 102804.

Wang, X., X. Lang, and D. Jiang. 2022. "Future Changes in Aridity in the Upper Indus Basin During the Twenty-First Century." *Climate Research* 87: 117–132.

Xu, X., X. Li, C. He, W. Tia, and J. Tian. 2022. "Development of a Simple Budyko-Based Framework for the Simulation and Attribution of ET Variability in Dry Regions." *Journal of Hydrology* 610: 127955.

Yang, Y.-C. E., C. Brown, W. Yu, J. Wescoat Jr., and C. Ringler. 2014. "Water Governance and Adaptation to Climate Change in the Indus River Basin." *Journal of Hydrology* 519: 2527–2537.

Yaseen, M., Y. Latif, M. Waseem, M. K. Leta, S. Abbas, and H. Akram Bhatti. 2022. "Contemporary Trends in High and Low River Flows in Upper Indus Basin, Pakistan." *Water* 14, no. 3: 337.

Zarch, M. A. A., B. Sivakumar, and A. Sharma. 2015. "Assessment of Global Aridity Change." *Journal of Hydrology* 520: 300–313.

Zhang, L., N. Potter, K. Hickel, Y. Zhang, and Q. Shao. 2008. "Water Balance Modeling Over Variable Time Scales Based on the Budyko Framework–Model Development and Testing." *Journal of Hydrology* 360, no. 1–4: 117–131.

Zhang, W., D. Zhao, and D. Liu. 2025. "Evaluation on Water Yield Service in Nansihu River Basin of China During the Recent 20 Years." *Environmental Earth Sciences* 84, no. 11: 296.

Supporting Information

Additional supporting information can be found online in the Supporting Information section. **Data S1:** joc70471-sup-0001-supinfo.docx. **Table S1:** Basin-scale hydrological variables derived using GPCC precipitation for the four Indus sub-basins, including precipitation (P), runoff (R), potential evapotranspiration (PET), and actual evapotranspiration ($AET = P - Q$). **Table S2:** Sensitivity analysis of projected actual evapotranspiration (AET) to ±10% perturbations in the Budyko parameter (ω), expressed as percentage change relative to the baseline ω simulation for near-term (2021–2040) and long-term (2081–2100) periods. **Figure S1:** Multi-model Q–Q plots of monthly precipitation for the Upper Indus, Kabul, Jhelum, and Chenab basins. The left and middle columns represent historical comparisons (raw vs. ERA5 and bias-corrected vs. ERA5) for 1962–2005, while the right column shows future comparisons (raw vs. bias-corrected) under RCP4.5. The 1:1 line indicates a perfect agreement. **Figure S2:** Same as Figure S1 but for RCP8.5.